ISBN: 978-1-925627-03-9

Culvert Baffles to Facilitate Upstream Fish Passage

Joseph Cabonce[1], Ramith Fernando[1], Hang Wang[2], Hubert Chanson[3]

[1]Research Student, The University of Queensland, School of Civil Engineering, Brisbane QLD, Australia

[2]Research Fellow, The University of Queensland, School of Civil Engineering, Brisbane QLD, Australia

[3]Professor, The University of Queensland, School of Civil Engineering, Brisbane QLD, Australia
E-mail: h.chanson@uq.edu.au

Abstract

This study investigates physically a new type of triangular corner baffles, aimed to facilitate the upstream passage of small-body fish typical of eastern Australian native fish species. Laboratory experiments were conducted in a large-size facility (12 m long, 0.5 m wide), in which detailed free-surface, velocity and boundary shear stress measurements were performed. The triangular baffles provided sizeable low-velocity regions and recirculation regions, suitable to facilitate upstream fish passage as well as rest areas. The hydrodynamics and flow resistance data in the barrel culvert showed a moderate decrease in discharge capacity for a given afflux. Energy dissipation took place as a combination of skin friction losses along the entire barrel and form losses behind each baffle.

1. INTRODUCTION

A culvert is a covered channel of relatively short length designed to pass floodwaters through or beneath an embankment, such as a roadway or railroad (Fig. 1). The design of a culvert is based upon hydrological, hydraulic, structural and geotechnical considerations. Altogether culverts may contribute about 15% of total road construction costs (Hee 1969). In terms of hydraulic engineering, the optimum size is the smallest barrel size allowing for inlet control operation (Herr and Bossy 1965, Chanson 2000a,2004). The culvert impact on the environment must also be taken into account. For the last three decades, the ecological impact of culverts on natural streams and rivers has been acknowledged (Behlke et al. 1991, Chorda et al. 1995). A number of national culvert design guidelines were developed to allow for upstream fish passage (Fairfull and Witheridge 2003, Hunt et al. 2012), too often leading to un-economical designs. While the culvert discharge capacity derives from hydrological and hydraulic engineering considerations, the final design results in large velocities in the barrel, creating some fish passage hindrance. Baffles may be installed along the barrel invert to provide some fish-friendly alternative (Olsen and Tullis 2013, Chanson and Uys 2016). But, traditional baffles can reduce significantly the culvert discharge capacity for a given afflux (Larinier 2002, Olsen and Tullis 2013), increasing drastically the total cost of the structure and roadway to achieve same discharge and afflux characteristics.

Chanson and Uys (2016) proposed a simple triangular corner baffle system, producing little reduction in discharge capacity while creating slow flow regions, suitable to assist small bodied fish passage in box culvert structures. The system was herein tested systematically in a near-full-scale physical facility. Tests were repeated with several configurations to ascertain potential scale effects as well as to determine the performances of baffled culvert barrel for a range of baffle size and spacing.

2. EXPERIMENTAL FACILITY AND PROCEDURE

New experiments were conducted in a 12 m long 0.5 m wide rectangular horizontal flume, supplied with fish-friendly waters, located at the University of Queensland. The horizontal slope was selected to

reduce the number of independent variables and to eliminate any gravity effect in relation to upstream fish passage. The channel boundaries consisted of smooth PVC bed and glass walls (Fig. 2). Both upstream and downstream stainless steel screens were installed to ensure the safety of small fish (Wang et al. 2016a). The facility size was comparable to a typical single-cell culvert structure in eastern Australia, and would correspond to a 1:2 scale model of a single cell of the structure seen in Figure 1.

The flow rate was measured with an orifice meter, designed based upon the British Standards and calibrated on site. The percentage of error was expected to be less than 2% on the discharge measurement. The water depths were measured using rail mounted pointer gauges with an accuracy of ±0.5 mm. Velocity and pressure measurements were conducted with a Prandtl-Pitot tube. The Pitot tube was a Dwyer® 166 Series Prandtl-Pitot tube with a 3.18 mm diameter tube made of corrosion resistant stainless steel. The translation of the Prandtl-Pitot probe in the vertical direction was controlled by a fine adjustment travelling mechanism connected to a Mitutoyo™ digimatic scale unit. The experiments were documented using a digital SLR camera Pentax™ K-3 as well as a digital camera Casio™ Exilim EX-10 with high-speed video capabilities.

Several configurations were tested. Reference experiments were performed with the smooth PVC invert and smooth sidewalls (Smooth boundary). Experiments were conducted with several types of isosceles triangular corner baffles (Fig. 2). The triangular baffles were fixed in the bottom left corner of the flume. Each baffle was an isosceles triangle with a 45° angle. Three different heights h_b were tested 0.033 m < h_b < 0.133 m and six different longitudinal spacing L_b were used for each baffle size 0.33 m < L_b < 2.0 m. A total of 18 configurations were tested with a constant baffle size and spacing for the whole channel length, for discharges between 0.0261 m^3/s and 0.0556 m^3/s.

Figure 1 – Three-cell standard box culvert outlet along Marom Creek beneath Bruxner highway B60, at Wollongbar NSW (Australia) on 28 October 2016.

2.1. Calibration of the Prandtl-Pitot tube

The Prandtl-Pitot tube was calibrated as a Preston tube to measure the skin friction shear stress at a wall, when the tube is in contact with the wall (Patel 1965). The concept is based upon dimensional and theoretical considerations. The calibration was conducted in open channel flows, yielding a monotonic relationship between the boundary shear stress and Pitot tube reading (Fig. 3). The data followed closely a solution of the Prandtl mixing length model in the wall region (Cabonce et al. 2017):

$$\tau_o = \rho \times \kappa^2 \times \frac{V_b^2}{N^2} \quad (1)$$

where τ_o is the local skin friction boundary shear stress, ρ is the fluid density, κ is the von Karman constant (κ = 0.4), N is the power law exponent, typically N = 7 for smooth turbulent flows, and V_b is the velocity measured by the Prandtl-Pitot tube lying on the boundary. The theoretical solution (Eq. (1)) is close to the calibration curves obtained by Patel (1965), Macintosh (1990) and Chanson (2000b), as illustrated in Figure 3.

The Prandtl-Pitot tube was further tested in negative flow regions. The dynamic head became smaller than the static head, when the dynamic tapping was in the wake of the tube. Despite some scatter caused by the very small pressure difference between the total and static tappings, the velocity and head difference were best correlated by:

$$V_x = -17.81 \times (-\Delta H)^{0.538} \quad (2)$$

where V is the velocity in m/s, ΔH is the difference between the total head and piezometric head in metres, and the normalised correlation coefficient is R = 0.801. Note that Equations (1) and (2) were developed for the Dwyer® 166 Series Prandtl-Pitot tube ($\varnothing$ = 3.18 mm). They should not be used with another tube without further validation tests.

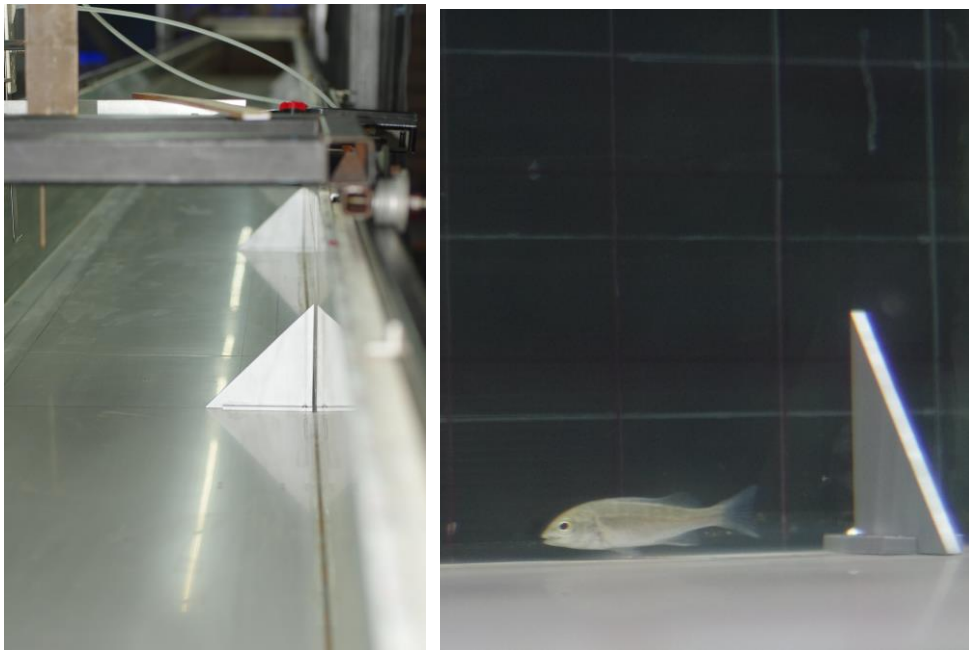

Figure 2 – Experimental channel - Left: h_b = 0.133 m, L_b = 1.33 m. Right: juvenile silver perch (*Bidyanus bidyanus*) resting in the stagnation zone upstream of a triangular baffle, h_b = 0.067 m, L_b = 0.67 m (flow direction from left to right).

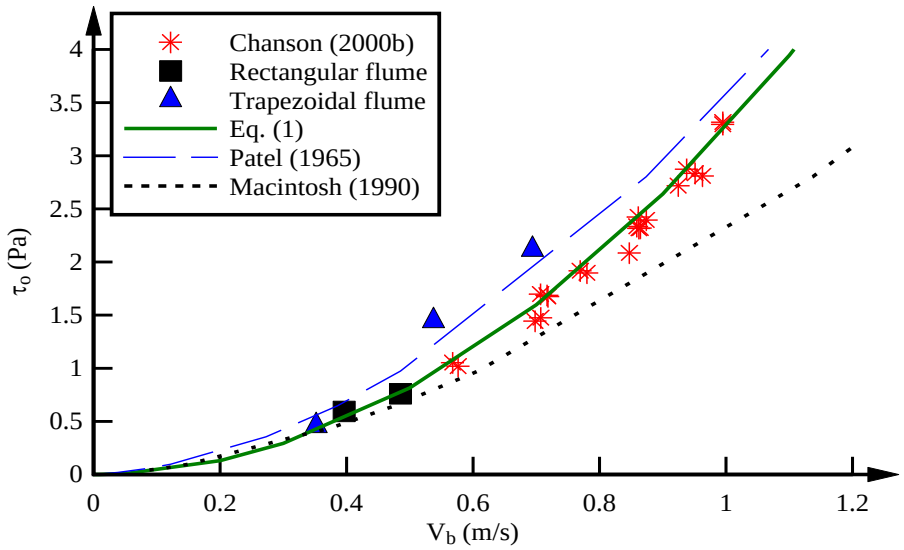

Figure 3 – Calibration curve of the Prandtl-Pitot tube for boundary shear stress measurements. Comparison with Equation (1) assuming N = 7 and Patel's (1965) correlation.

3. BASIC FLOW PATTERNS

At the upstream end of the flume, the flow was quasi-uniform with thin sidewall and bed boundary layers. With increasing longitudinal distance, a bottom boundary layer developed. In the smooth boundary configuration, the outer edge of the developing boundary layer interacted with the free-surface for x > 4 to 6 m depending upon the flow rate (Wang et al. 2016a). With the triangular baffle configurations, the flow was three-dimensional as a result of the turbulence generated by the baffles, and the flow became fully-three-dimensional for x > 4 m. In the following section, the focus is on the fully-developed flow region (x > 4-6 m). For all flow conditions, the free-surface was relatively smooth along the flume. The water surface elevation decreased with increasing distance, as a H2 backwater profile. The data showed however a local increase in depth towards the downstream end of the flume, caused by the presence of the downstream screen and associated localised head loss. For the largest baffles, the free-surface presented some localised dip immediately downstream of each baffle next to the left sidewall. This dip phenomenon was localised next to the left sidewall, and is believed to be linked to local flow separation in the near-wake of the baffle, associated with a local fluid acceleration and associated pressure reduction, according to ideal-fluid flow theory.

Recirculation visualisations were conducted using dye injection. The observations showed the flow separation taking place at each baffle outer edge, with a region of local flow acceleration, a shear zone and recirculation region in the wake of the baffle. Several flow features were identified between successive baffles, as sketched in Figure 4 with coloured sections and arrows. The bulk of the flow took place for $y/(B-h_b) < 1$, where y is the transverse distance measured from the right sidewall and B the channel width (Zone 1). No recirculation or flow reversal was observed. At the triangular baffle edge, a shear zone (Zone 2) developed and momentum was transferred from the main stream to the recirculation zone behind the baffle (Zone 3). Behind each baffle, a primary zone of flow reversal (Zone 3) was observed, where the water flowed in the negative direction. Such a recirculation region may serve as rest areas for fish (Cahoon et al. 2007, Olsen and Tullis 2013), although the such an abrupt change in flow direction might disturb some fish. At the downstream end of the recirculation region, the re-attachment region (Zone 3.5) was characterised by a highly turbulent motion with a time-averaged longitudinal velocity about zero. The length of the re-attachment region ranged from 0.05 m for medium baffles (h_b = 0.067 m) to 0.05-0.1 m for large baffles (h_b = 0.133 m). Further downstream and immediately upstream of each baffle, a stagnation region was observed (Zone 4). This region was characterised by a change in fluid direction, as the streamlines spread around the baffle, and locally the fluid velocity was small (Fig. 2B). Overall the observations indicated that the cross-sectional averaged velocity and baffle spacing had little effect on the recirculation pattern. The baffle size increased the flow reversal region, particularly its longitudinal size, while the stagnation region became more pronounced for the largest baffle size.

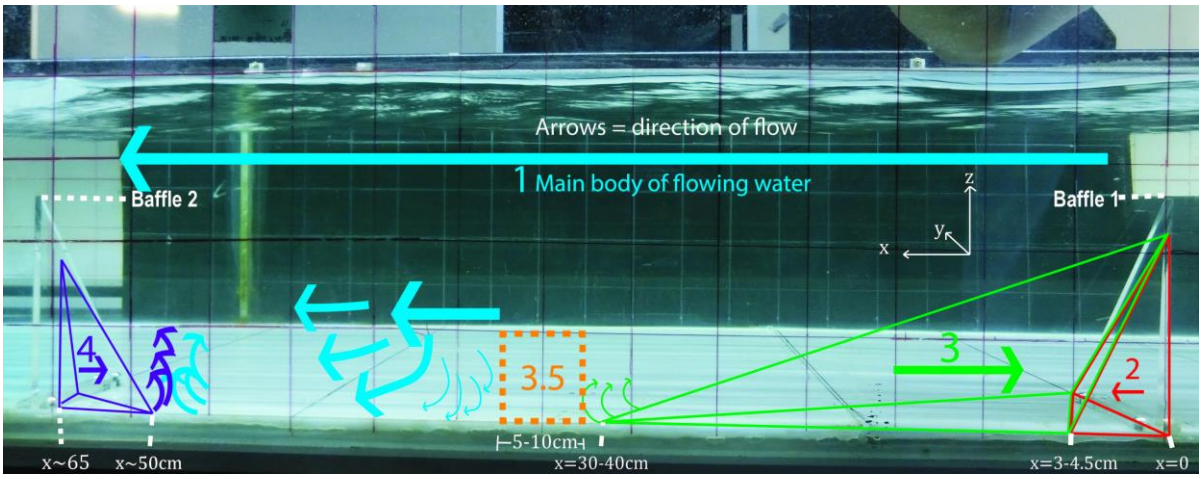

Figure 4 – Flow patterns and recirculation motion between two successive baffle along the left sidewall for the largest baffles (h_b = 0.133 m). Flow direction from right to left.

The flow resistance of the triangular baffle configurations was tested and compared to the smooth boundary channel data. The spatially-averaged boundary shear stress was deduced from the measured free-surface profiles and estimated friction slopes for x > 5 m. Present results are presented in Figure 5 in terms of the Darcy-Weisbach friction factor, where D_H is the hydraulic diameter and Re is the Reynolds number defined in terms of the cross-sectional averaged velocity and hydraulic diameter. The smooth boundary configuration results were very close to smooth turbulent flow results (Schlichting 1979). Figure 5 illustrates the effect of relative baffle height h_b/D_H: the data showed an increasing friction factor with increasing relative baffle height for a given baffle spacing. Overall the presence of triangular baffles had a moderate effect on the flow resistance, as reported by Chanson and Uys (2016) in a small-size laboratory model. Herein the Darcy-Weibach friction factor data for the triangular baffle channel were best correlated by:

$$f = f' + 0.285 \times \left(\frac{h_b^4}{L_b \times B^2 \times d} \right)^{0.401} \quad (3)$$

where d is the flow depth and f' is the smooth turbulent flow friction factor calculated using the Karman-Nikuradse formula. Equation (3) was compared successfully to the experimental data, with a normalised correlation coefficient of 0.936 and a standard error of 0.000854.

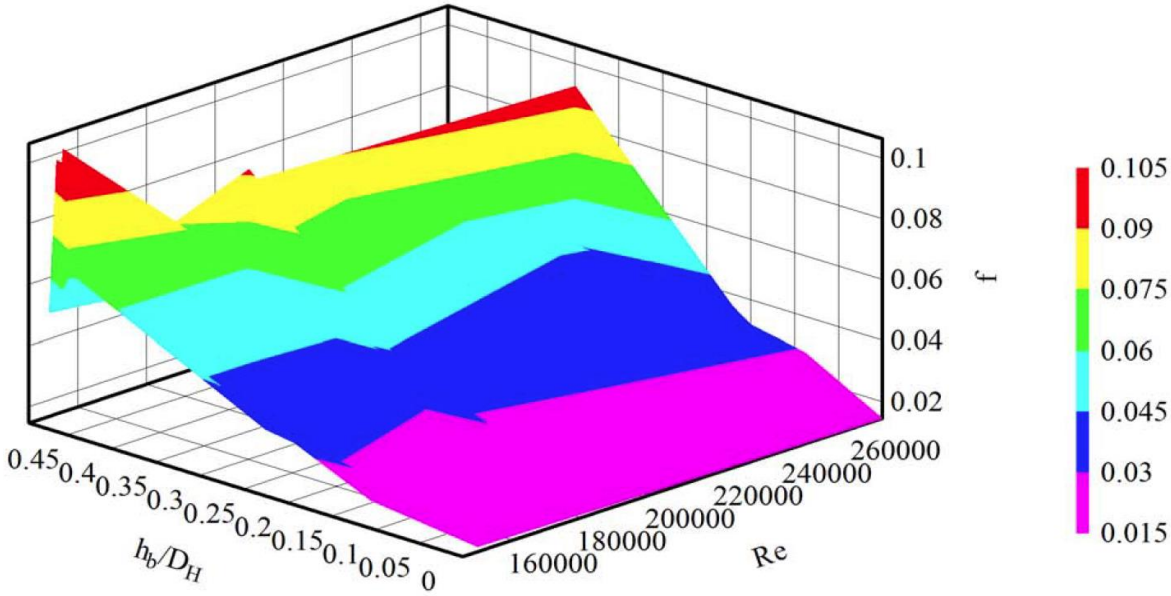

Figure 5 – Darcy-Weisbach friction factor f (coloured legend, far right) as a function of the Reynolds number Re and relative baffle height h_b/D_H.

4. VELOCITY MEASUREMENTS

In the smooth channel, the velocity distributions were reasonably symmetrically distributed about the channel centreline. In the presence of triangular baffles at the bottom left corner, the flow was markedly asymmetrical and the velocity field was skewed, with larger velocities and velocity gradients towards the right half of the channel. This was clearly evidenced by velocity measurements, with some complicated flow pattern next to the left corner (Fig. 6). Figure 6 shows typical time-averaged longitudinal velocity contours for the baffled channel. In Figure 6, X is the relative distance between two successive baffles: $X = (x-x_b)/L_b$, with L_b the baffle spacing and x_b the position of the lead baffle. In each contour plot, the left axis corresponds to the smooth right wall and the right axis to the left wall, where the baffles were located. Immediately downstream of a baffle, the near-wake region was characterised by some negative flow motion close to the bottom left corner. This is seen in Figure 6 (Top right). With increasing relative distance from the lead baffle, the left corner region remained affected by some slow flow motion. Some flow concentration was also observed towards the right channel side, with a thinner right sidewall boundary layer region, and a slow-velocity region close to the left sidewall and corner region. The resulting flow motion led to a complicated secondary flow pattern.

The skin friction resistance was measured using the Prandtl-Pitot tube, based upon Equation (1). The data showed that the skin friction shear stress was symmetrically distributed about the channel centreline, for the smooth boundary channel. In presence of corner baffles, the skin friction shear stress was larger towards the right sidewall (Fig. 7). Typical results are shown in Figure 7, in the form of a contour plot of the dimensionless skin friction shear stress on the bed, i.e. the ratio of skin friction shear stress to total boundary shear stress. For the triangular baffle channel, the skin friction boundary shear stress was less than the total boundary shear stress. The data were spatially-averaged over a longitudinal baffle spacing. Depending upon the baffle configuration (size, spacing) and flow rate, the ratio of skin friction resistance to total flow resistance f_{skin}/f ranged from 0.21 to 0.58.

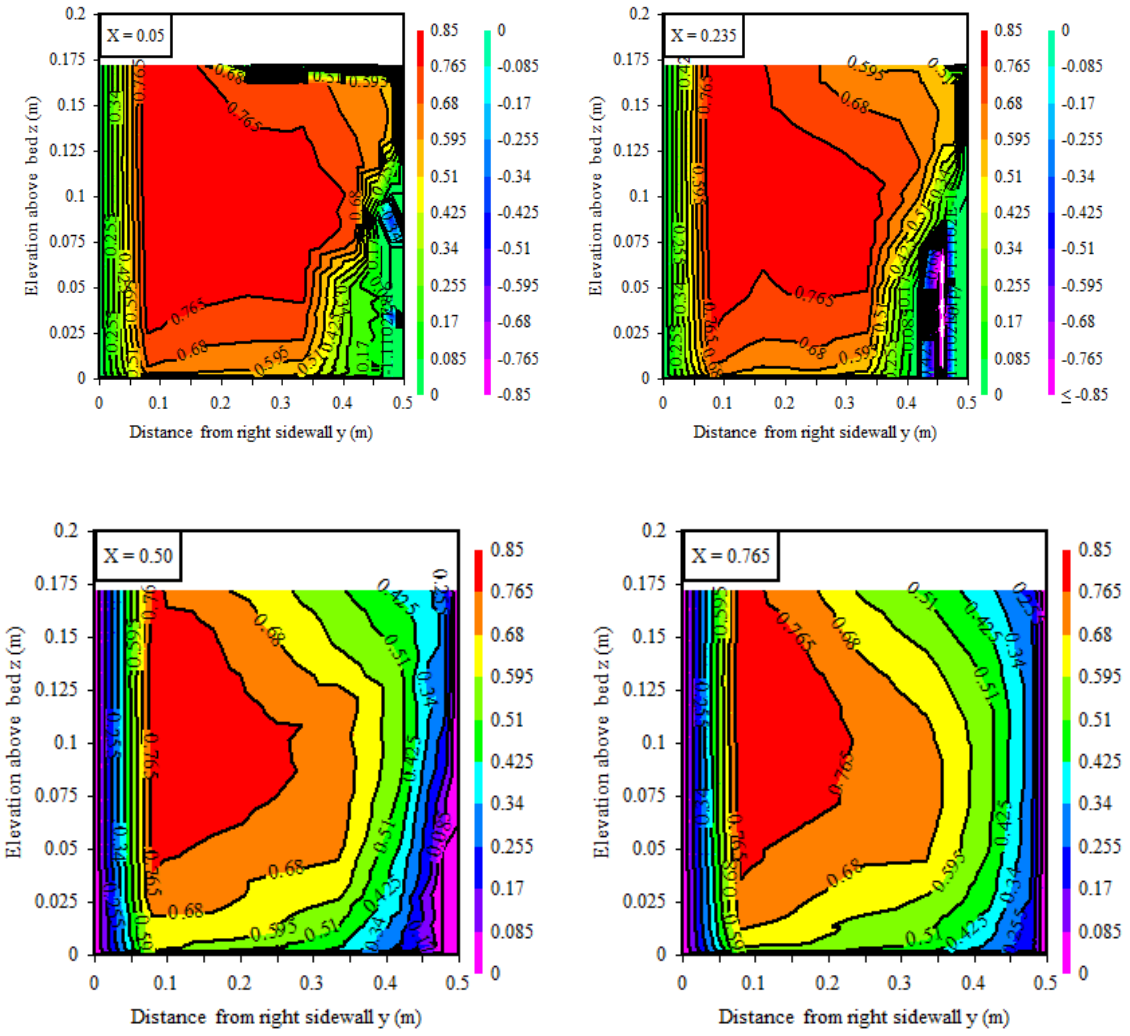

Figure 6 – Contour plots of time-averaged longitudinal velocity V_x (in m/s) - Q = 0.0556 m³/s, d = 0.173 m, h_b = 0.133 m, L_b = 0.67 m, x_b = 8.12 m - From left to right, top to bottom: x = 8.152 m, 8.275 m, 8.45 m & 8.625 m (X = 0.05, 0.235, 0.50 & 0.765).

5. CONCLUSION

A simple triangular corner baffle system was developed for standard box culverts, producing little reduction in discharge capacity while creating slow flow regions upstream and downstream of baffles. Such a basic design may assist with the upstream passage of small body mass fish in culvert structures on very flat bed slope. The system was herein tested systematically in a near-full-scale physical facility, 0.5 m wide and 12 m long. The results may be extrapolated to larger culvert structures based upon a Froude similitude. The observations indicated several key flow features between successive baffles. These included flow separation immediately downstream of the inclined edge of the triangular baffle, followed by a shear zone. The presence of triangular baffles had a moderate effect on the flow resistance, albeit the data indicated the combined effect of relative baffle height and spacing on the friction factor.

While, in the smooth boundary channel, 5-10% of the flow area experienced time-averaged velocities less than $0.5 \times V_{mean}$, where V_{mean} is the bulk velocity, this relative surface area was considerably larger in the triangular baffle channel, with 10-25% of the flow area experiencing $V_x < 0.5 \times V_{mean}$, depending upon the flow rate and baffle configuration. The results indicated that the presence of triangular baffles increased the relative size of slow-flow regions, by a factor two to three. Such low velocity regions are preferential swimming zones for fish (Lupandin 2005), and should be favourable to small-bodied fish passage, since these fish tend to prefer to swim next to sidewalls and flume corners (Wang et al.

2016b). The findings confirmed the limited field observations in a box culvert equipped with a different type of corner baffles (Quadrio 2007)

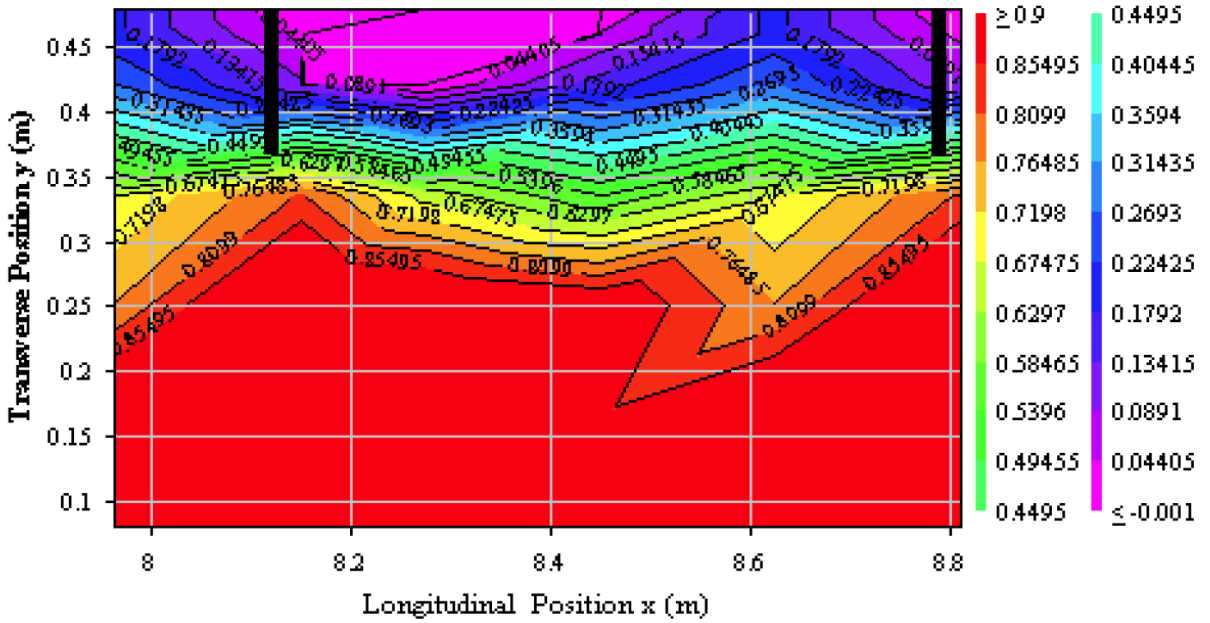

Figure 7 – Contour plots of relative bed (skin friction) boundary shear in triangular baffle channel. Flow direction from left to right, x_b = 8.12 m, Q = 0.0556 m^3/s, h_b = 0.133 m, L_b = 0.67 m. Solid black lines are triangular baffles (x_b = 8.12 m & 8.79 m).

6. ACKNOWLEDGMENTS

The authors acknowledge the helpful assistance of Jee Sam Tiew, Jui Jie Tan, Angela Arum, Michael Cheung and Thi My Tram (Stephanie) Ngo (The University of Queensland, Australia) in collecting physical data. They thank Xinqian (Sophia) Leng and Urvisha Kiri (The University of Queensland, Australia) for their inputs. The authors acknowledge the technical assistance of Jason Van Der Gevel and Stewart Matthews (The University of Queensland). The financial support through the Australian Research Council (Grant LP140100225) is acknowledged.

7. REFERENCES

Behlke, C.E., Kane, D.L., McLeen, R.F., and Travis, M.T. (1991). *Fundamentals of Culvert Design for Passage of Weak-Swimming Fish*. Report FHW A-AK-RD-90-10, Department of Transportation and Public Facilities, State of Alaska, Fairbanks, USA, 178 pages.

Cabonce, J., Fernando, R., Wang, H., and Chanson, H. (2017). *Using Triangular Baffles to Facilitate Upstream Fish Passage in Box Culverts: Physical Modelling*. Hydraulic Model Report No. CH107/17, School of Civil Engineering, The University of Queensland, Brisbane, Australia, 130 pages.

Cahoon, J.E., McMahon, T., Solcz, A., Blank, M., and Stein, O. (2007). *Fish Passage in Montana Culverts: Phase II - Passage Goals*. Report FHWA/MT-07-010/8181, Montana Department of Transportation and US Department of Transportation, Federal Highway Administration, 61 pages.

Chanson, H. (2000a). *Introducing Originality and Innovation in Engineering Teaching: the Hydraulic Design of Culverts*. European Journal of Engineering Education, 25 (4), 377-391.

Chanson, H. (2000b). *Boundary Shear Stress Measurements in Undular Flows: Application to Standing Wave Bed Forms*. Water Resources Research, 36 (10), 3063-3076.

Chanson, H. (2004). *The Hydraulics of Open Channel Flow: An Introduction*. Butterworth-Heinemann, 2nd edition, Oxford, UK, 630 pages.

Chanson, H., and Uys, W. (2016). *Baffle Designs to Facilitate Fish Passage in Box Culverts: A Preliminary Study*. in Crookston, B., Tullis, B. (Eds), Proceedings of 6th IAHR International Symposium on Hydraulic Structures, 27-30 June, Portland OR, USA, pp. 295-304.

Chorda, J., Larinier, M., and Font, S. (1995). *Le Franchissement par les Poissons Migrateurs des Buses et Autres Ouvrages de Rétablissement des Ecoulements Naturels lors des Aménagements Routiers et Autoroutes*. Etude Expérimentale. Rapport HYDRE n°159 - GHAAPPE n°95-03, Service d'Etudes Techniques des Routes et Autoroutes, Toulouse, France, 116 pages (in French).

Fairfull, S., and Witheridge, G. (2003). *Why do fish need to cross the road?* Fish passage requirements for waterway crossings. NSW Fisheries, Cronulla NSW, Australia, 14 pages.

Hee, M. (1969). Hydraulics of Culvert Design Including Constant Energy Concept. Proc. 20th Conf. of Local Authority Engineers, Dept. of Local Govt, Queensland, Australia, paper 9, pp. 1-27.

Henderson, F.M. (1966). *Open Channel Flow*. MacMillan Company, New York, USA.

Herr, L. A., and Bossy, H.G. (1965). *Hydraulic Charts for the Selection of Highway Culverts*. Hydraulic Engineering Circular, US Dept. of Transportation, Federal Highway Admin., HEC No. 5, December.

Hunt, M., Clark, S., and Tkach, R. (2012). *Velocity Distributions near the Inlet of Corrugated Steep Pipe Culverts*. Canadian Journal of Civil Engineering, 39, 1243-1251.

Larinier, M. (2002). *Fish Passage through Culverts, Rock Weirs and Estuarine Obstructions*. Bulletin Français de Pêche et Pisciculture, 364 (18), 119-134.

Lupandin, A.I. (2005). *Effect of flow turbulence on swimming speed of fish*. Biology Bulletin, 32 (5), 461-466.

Macintosh, J.C. (1990). Hydraulic Characteristics in Channels of Complex Cross-Section. *Ph.D. thesis*, University of Queensland, Department of Civil Engineering, Australia, November, 487 pages.

Olsen, A. and Tullis, B. (2013). *Laboratory Study of Fish Passage and Discharge Capacity in Slip-Lined, Baffled Culverts*. Journal of Hydraulic Engineering, ASCE, 139 (4), 424–432.

Patel, V.C. (1965). *Calibration of the Preston Tube and Limitations on its use in Pressure Gradients*. Journal of Fluid Mechanics, 23 (Part 1), 185-208.

Quadrio, J. (2007). *Passage of Fish Through Drainage Structures*. Queensland Roads, Sept., 6-17.

Schlichting, H. (1979). *Boundary Layer Theory*. McGraw-Hill, New York, USA, 7th edition.

Wang, H., Beckingham, L.K., Johnson, C.Z., Kiri, U.R., and Chanson, H. (2016a). *Interactions between Large Boundary Roughness and High Inflow Turbulence in Open channel: a Physical Study into Turbulence Properties to Enhance Upstream Fish Migration*. Hydraulic Model Report No. CH103/16, School of Civil Engineering, The University of Queensland, Brisbane, Australia, 74 pages.

Wang, H., Chanson, H., Kern, P., and Franklin, C. (2016b). *Culvert Hydrodynamics to enhance Upstream Fish Passage: Fish Response to Turbulence*. in Ivey, G., Zhou, T., Jones, N., Draper, S. (Eds), Proceedings of 20th Australasian Fluid Mechanics Conference, Australasian Fluid Mechanics Society, Perth WA, Australia, 5-8 December, Paper 682, 4 pages.